Journal of Visualized Experiments

Whole Body and Regional Quantification of Active Human Brown Adipose Tissue Using 18F-FDG PET/CT

--Manuscript Draft--

Article Type:	Methods Article - JoVE Produced Video
Manuscript Number:	JoVE58469R1
Full Title:	Whole Body and Regional Quantification of Active Human Brown Adipose Tissue Using 18F-FDG PET/CT
Keywords:	Brown Fat; PET/CT; brown adipose tissue; cold-activation; Fluorodeoxyglucose; image processing; Obesity; Diabetes; thermoregulation
Corresponding Author:	Brooks Leitner National Institute of Diabetes and Digestive and Kidney Diseases Bethesda, MD UNITED STATES
Corresponding Author's Institution:	National Institute of Diabetes and Digestive and Kidney Diseases
Corresponding Author E-Mail:	brooks.leitner@nih.gov
Order of Authors:	Katherine I Kim
	Shan Huang
	Laura A Fletcher
	Alana E O'Mara
	Ilan Tal
	Robert J Brychta
	Aaron M Cypess
	Kong Y Chen
	Brooks Leitner
Additional Information:	
Question	**Response**
Please indicate whether this article will be Standard Access or Open Access.	Open Access (US$4,200)
Please indicate the **city, state/province, and country** where this article will be **filmed**. Please do not use abbreviations.	9000 Rockville Pike 10-CRC Room 5-3635, Bethesda, MD 20892

TITLE:

Whole Body and Regional Quantification of Active Human Brown Adipose Tissue Using ^{18}F-FDG PET/CT

AUTHORS AND AFFILIATIONS:

Katherine Kim[1], Shan Huang[2], Laura A. Fletcher[1], Alana E. O'Mara[1], Ilan Tal[3], Robert J. Brychta[1], Aaron M. Cypess[1], Kong Y. Chen[1], Brooks P. Leitner[1]*

[1]Diabetes, Endocrinology, and Obesity Branch, National Institute of Diabetes and Digestive and Kidney Diseases, National Institutes of Health, Bethesda, MD

[2]National Cancer Institute, National Institutes of Health, Bethesda, MD

[3]Division of Nuclear Medicine and Molecular Imaging, Department of Radiology, Beth Israel Deaconess Medical Center, Harvard Medical School, Boston, MA

Corresponding Author:

Brooks P. Leitner (Brooks.leitner@yale.edu)

Email Addresses of Co-authors:

Katherine Kim (kkim2209@umd.edu)
Shan Huang (shan.huang2@nih.gov)
Laura Fletcher (laura.fletcher@nih.gov)
Alana O'Mara (Alana.o'mara@nih.gov)
Ilan Tal (ilan.tal@gmail.com)
Robert Brychta (brychtar@niddk.nih.gov)
Aaron Cypess: (aaron.cypess@nih.gov)
Kong Chen (kong.chen@niddk.nih.gov)

KEYWORDS:

Brown adipose tissue, cold-activation, adult human, fluorodeoxyglucose, positron emission tomography, computed tomography, obesity, thermoregulation

SUMMARY:

Using free, open-source software, we have developed an analytical approach to quantify total and regional brown adipose tissue (BAT) volume and metabolic activity of BAT using ^{18}F-FDG PET/CT.

ABSTRACT:

In endothermic animals, brown adipose tissue (BAT) is activated to produce heat for defending body temperature in response to cold. BAT's ability to expend energy has made it a potential target for novel therapies to ameliorate obesity and associated metabolic disorders in humans. Though this tissue has been well studied in small animals, BAT's thermogenic capacity in humans remains largely unknown due to the difficulties of measuring its volume, activity, and

distribution. Identifying and quantifying active human BAT is commonly performed using ^{18}F-Fluorodeoxyglucose (^{18}F-FDG) positron emission tomography and computed tomography (PET/CT) scans following cold-exposure or pharmacological activation. Here we describe a detailed image-analysis approach to quantify total-body human BAT from ^{18}F-FDG PET/CT scans using an open-source software. We demonstrate the drawing of user-specified regions of interest to identify metabolically active adipose tissue while avoiding common non-BAT tissues, to measure BAT volume and activity, and to further characterize its anatomical distribution. Although this rigorous approach is time-consuming, we believe it will ultimately provide a foundation to develop future automated BAT quantification algorithms.

INTRODUCTION:

The increasing prevalence of obesity worldwide[1] has prompted an investigation into novel therapeutics to prevent and ameliorate obesity and its associated complications. Obesity is due in part to excess energy stored in white adipose tissue (WAT) in the form of triglycerides[2]. Brown adipose tissue (BAT) differs from WAT most notably due to its higher mitochondrial content, smaller and multilocular lipid droplets, distinct anatomical distribution, greater sympathetic innervation, and heat generating ability. Although BAT was once thought to exist only in small mammals and newborn infants, the presence of functional BAT was confirmed in adult humans in 2009[3–5]. The thermogenic capacity of human BAT is not yet known, but extensive study in small animals has shown that non-shivering thermogenesis can constitute up to 60% of their metabolism during cold-exposure[6]. As a result, human BAT is now being explored as a target for the treatment and prevention of obesity and related disorders[7]. Several clinical studies have shown that BAT thermogenesis correlates with increased glucose uptake and energy expenditure upon activation by mild cold exposure[8–10]. Yet, BAT's contribution to cold-induced thermogenesis remains controversial[11–14], with much debate centered around how to quantify human BAT[15]. To better understand if BAT thermogenesis can be harnessed to combat obesity, it is critical to have an accurate measurement of its volume and metabolic activity.

Obtaining precise measurements of BAT is challenging due to BAT's unique anatomical distribution in humans. BAT is distributed within the white adipose depots in the neck, thorax, and abdomen in sites that are inaccessible to uncomplicated biopsies[14]. Autopsies have been used to characterize BAT anatomically[16], but are infeasible for most research laboratories doing large studies and cannot provide longitudinal or functional information. Since BAT has a similar density to WAT and can occur in narrow fascial layers or in small pockets interspersed with WAT[16], it is difficult to identify using a single, conventional imaging technique. This heterogeneity also makes automatic quantification of BAT more difficult than quantification of homogenous structures such as the liver[17].

To overcome these challenges, BAT volume and activity are commonly quantified by coupling computed tomography (CT) and positron emission tomography (PET). The radiolabeled glucose analog ^{18}F-Fluourodeoxyglucose (^{18}F-FDG) is the most widely used tracer to study BAT metabolic activity[18]. Adipose tissue can be differentiated from other tissue and air based on density information provided by the CT image in Hounsfield units (HU). PET images show the

amount of ^{18}F-FDG taken up into a volume of tissue in units of standardized uptake values (SUV). Active BAT can be separated from tissue with insignificant tracer uptake, including WAT and inactive BAT, by co-registering PET images with corresponding CT scans and choosing an appropriate SUV threshold.

Through this paper, we aim to provide a step-by-step approach with an instructional video that can be used by clinical researchers to quantify human BAT using ^{18}F-FDG PET/CT scans. This image analysis technique is ideally used after subject(s) have been exposed to cold or treated with pharmacological BAT stimulants. Specifically, we demonstrate to users on how to construct regions of interest (ROIs) while minimizing false positives using a free, open-source image-processing software (ImageJ) with a specific plug-in (petctviewer.org). The result of this approach can be used to study BAT volume, activity (glucose uptake), and anatomical distribution in individual study subjects.

PROTOCOL:

All PET/CT images shown in this manuscript were obtained from participants in National Institutes of Health protocol no. 12-DK-0097 (ClinicalTrials.gov identifier NCT01568671). All participants provided written informed consent, and all experiments were approved by the Institutional Review Board of the National Institute of Diabetes and Digestive and Kidney Diseases.

1. Software Installation

1.1. Download ImageJ from *imagej.net* or use the link in *petctviewer.org* to download Fiji.

Note: The 64-bit version of ImageJ is required for sets with over 1000 images.

1.2. Download and apply the PET/CT Viewer Plug-in to ImageJ following the installation instructions on *petctviewer.org*. Refer to this website for a comprehensive guide to PET/CT Viewer, and be sure to check for regular updates to the software and the link to general instructions (http://sourceforge.net/p/bifijiplugins/wiki/Brown%20fat%20Volume/).

2. Loading PET/CT Images

2.1. Upload the following three stacks of images into the PET/CT Viewer Plug-in: attenuation corrected PET (CPet), non-attenuation corrected PET (UPet), and attenuation corrected CT (CT). Upload images using one of two methods (**Figure 1**).

2.1.1. Method 1: Drag-and-drop

2.1.1.1. Drag-and-drop from file explorer CT, CPet, and UPet filesets.

2.1.1.2. Click “yes” on the three prompts that appear (Open all X images in “folder” as a stack),

leaving the checkboxes within the prompts unchecked.

2.1.1.3. When all three image sets are loaded, go to the ImageJ toolbar, select “plug-ins”, and scroll down the drop-down menu to select “Pet-ct viewer”.

2.1.2. Method 2: Read Studies from CD or location on disk:

2.1.2.1. Assign a location name to the dataset in the “Setup” tab. Assign a “DICOM path” by clicking “Browse” and navigating to a high-level storage folder containing all image sets.

Note: DICOM (Digital Imaging and Communications in Medicine) is a file format commonly used for medical images and the “DICOM path” refers to the set of folders that contains all raw DICOM images.

2.1.2.2. Return to the “Read” tab where individual scans (from one subject and one date) will become selectable for image processing.

2.1.2.3. Select the subject, press “Read,” and ImageJ will automatically upload all three associated sets and launch the PET/CT viewer.

2.2. Load a previously made set of ROIs back into the PET/CT viewer by clicking the “load” button on the “Brown fat, ROIs” editor.

Note: ImageJ will only allow an ROI .csv file created from the current set of CT, CPET, and UPET images to be loaded.

3. Navigating the PET/CT Viewer Plug-in

3.1. Wait for the PET/CT viewer to appear after loading as a new window with three separate views of the PET/CT images, presented either individually or fused.

3.1.1. Click the “MIP” button at the top left of the PET/CT viewer to replace one of the other two windows with a fused PET/CT view. However, if this button is only clicked once, the MIP will no longer be available.

Note: The MIP or maximal intensity projection is a two-dimensional, full body image displaying only the pixels with highest intensity in each axial slice.

3.1.2. Click the “MIP” button again to bring back the MIP; now views of the fused PET/CT, CT, and MIP should be available.

3.2. Switch the MIP image orientation with the “>>”, “F”, and “S” buttons at the top of the PET-CT viewer.

3.3. Change the orientation of the PET, CT, and fused PET/CT images to axial, coronal, or sagittal planes using the three buttons to the left of the magnifying glass.

3.4. Click on the magnifying glass on the toolbar at the top of the PET-CT viewer to switch the function of the mouse's scroll wheel.

3.4.1. Zoom in on all views (except the MIP) by scrolling with the magnifying glass selected.

3.4.2. Navigate through slices on all views (except the MIP) by scrolling when the magnifying glass is not selected.

Note: Clicking on the MIP will also change the PET and CT slices to the anatomical location at the level of the cursor.

3.5. Select "Edit" at the top left of the toolbar and select "Brown fat, ROIs" from the dropdown menu that appears. A new dialog box will appear. Make sure that the following options are selected before starting quantification:

3.5.1. Check the "Use SUV" and "Use CT" checkboxes.

3.5.2. Select one of the three voxel inclusion criteria ("Any", "Average", or "All").

Note: "Any" was used in Leitner *et al.* 2017[19]. For a detailed explanation of other options, refer to petctviewer.org.

3.5.3. Select "Interior" to apply the BAT detection algorithm to examine the voxels inside (rather than outside) the area of the ROI.

3.6. Input SUV limits for BAT in the first row of free-text fields of this dialog box.

3.6.1. Input an SUV lower limit normalized to the individual's measured or predicted lean body mass and an upper limit sufficient to accommodate high activity levels[19,20].

Note: BAT maximal SUVs as high as ~75 g/mL have been reported in previous studies[17]; thus, 100 g/mL is a reasonable upper limit.

3.7. Input the BAT density range in the second row of free-text fields.

Note: A -300 HU lower limit and -10 HU upper limit were used in Leitner *et al.* 2017[19] and a range from -190 to -10 HU was also previously recommended[21].

3.8. Check the checkbox located beneath "Vol*mean" so that all voxels deemed to be BAT will be highlighted in blue while the "brown fat, ROI" window is open.

Note: The SUVmax will appear in red and the adjustable number next to this checkbox dictates the thickness of the highlight.

3.9. Draw the ROIs

3.9.1. Click the "Draw" button in the "brown fat, ROI" dialog box. All clicks made within the PET/CT viewer window will be considered points that make up ROIs.

3.9.1.1. Click anywhere within one of the three views to begin drawing an ROI.

Note: A minimum of three points is required to form an ROI. Double-click after the first or second point to automatically delete the points and leave ROI drawing mode.

3.9.1.2. Close and store the ROI by double-clicking after defining more than two points.

3.10. Compiling ROIs to obtain total BAT volume

3.10.1. Draw ROIs in the axial plane to obtain total BAT volume.

Note: It is easiest to have a maximum of one ROI per axial slice. Including more than one ROI per slice may lead to inadvertent overlap. Voxels identified as BAT in overlapping regions would then be counted more than once toward total BAT volume.

3.10.2. Set the starting and ending "slice limit" to the same slice, so that the ROI will only apply to the current axial slice (*e.g.* starting slice = 90 and ending slice = 90).

3.10.3. Circle one depot of BAT (*e.g.* in the left supraclavicular region) without completing the ROI. Continue the ROI by extending a connecting line across the body to the distant segment of BAT. Enclose the second BAT depot and double click on the previously identified point at the start of the 2nd region. Adjust ROI points as necessary to further reduce the possibility of false positives.

3.10.4. Label the ROI based on the anatomical level for future reference using the text box at the bottom left of the dialog box.

3.11. Deleting unwanted ROIs

3.11.1. Remove an unwanted ROI right after completion.

3.11.1.1. Double-click anywhere within the PET/CT viewer to complete the unwanted ROI.

3.11.1.2. Click the button with the recycling bin icon in the "Brown fat, ROI" dialog box.

3.11.1.3. Click "yes" when prompted whether or not the user wishes to remove the current ROI.

3.11.2. Delete a previously-made ROI.

3.11.2.1. Select the desired ROI using the up or down arrows next to the ROI number.

3.11.2.2. Click the recycling button.

Note: Once the ROI has been deleted, the numbers associated with each ROI greater than the deleted ROI will accordingly shift down in order (*e.g.* if ROI #2 is deleted, ROI #3 will become #2, and ROI #4 will become #3, and so on). Labeled ROIs make this process easier.

3.12. Saving ROIs

3.12.1. Click the "Save" button and provide a file name to save completed ROIs in a .csv file.

Note: It is recommended that ROIs be saved in intervals of 10 slices so that progress is not lost. The .csv files can be opened in a text editor or spreadsheet program and contains all relevant data about identified BAT in each ROI including volume, activity, SUVmean, *etc.* Changing values in a spreadsheet program may alter the file format and make it unreadable in ImageJ.

4. Quantifying whole-body BAT

4.1. Use these general guidelines to identify BAT in all regions of the body.

4.1.1. Avoid sections of bordering tissue with high density or activity contrasts, as minute co-registration issues may introduce false positives.

Note: Keep in mind that BAT depots are often symmetrical, a property that will aid in visual BAT identification.

4.2. Use unique anatomical landmarks such as vertebral shape, other bony structures, and the presence of organs to identify the current anatomical region. Avoid region-specific structures known to produce false-positives.

4.2.1. Identify BAT in the cervical region (vertebrae C3-C7).

4.2.1.1. Navigate to the axial view at the third cervical vertebra (C3).

Note: C1-C2 regions may also contain BAT, but BAT detection is likely to be confounded by high uptake of FDG in brain and skeletal muscle.

4.2.1.2. Begin the ROI on the lateral side of the adipose tissue depot, avoiding neck muscles around the spinous process of the vertebra, and creating a border just posterior to the lower edge of the mandible.

4.2.1.3. Exclude the thyroid, which may have similar density and activity level as BAT (**Figures 2A and 2B**).

4.2.2. Identify BAT in the dorsocervical region (Vertebrae C5-C7).

4.2.2.1. Include this small, subcutaneous depot of BAT.

Note: It appears symmetrically within the subcutaneous fat of the back near C5-C7, **Figure 2B**.

4.2.2.2. Carefully include subcutaneous adipose tissue only where metabolic activity occurs.

4.2.3. Identify BAT in the supraclavicular region (Vertebrae C7-T3; Anterior to Spine, Posterior to Mediastinum)

4.2.3.1. Begin drawing the ROI one side most superficial, close to the highly active BAT region.

Note: BAT may extend to the area around the head of the humerus.

4.2.3.2. Avoid the area directly above the trachea, which contains the thyroid, and enclose the ROI so that false positives near the neck muscles and lungs are excluded.

4.2.4. Identify BAT in the axillary region (Vertebrae T3-T7).

4.2.4.1. Find axillary BAT as a progression from the supraclavicular region.

4.2.4.2. Select BAT near where the arm begins to separate from the torso, but avoid ribs and the lungs.

Note: These fat depots will eventually transition to subcutaneous WAT on the midaxillary line.

4.2.5. Identify BAT in the mediastinal region (Vertebrae T1-T7; Anterior):

Note: BAT may accumulate around the entirety of the sternum for some individuals.

4.2.5.1. Select BAT where the sternum begins to appear at the beginning of T2 near the anterior-most region of the individual's thoracic cavity, and continue ROIs inferiorly until the end of the xiphoid process.

4.2.6. Identify BAT in the paraspinal region (Vertebrae T1-T12), by drawing ROIs around BAT surrounding the body, not the spinous process, of the vertebra.

4.2.6.1. Begin including paraspinal BAT from the appearance of the first rib at the lower edge of C7.

4.2.6.2. Do not include areas between ribs, where intercostal muscles are localized.

4.2.7. Identify BAT in the abdominal region (Inferior to T12).

4.2.7.1. Avoid the ureters, which have a similar density to BAT and very high activity levels. (**Figure 2D**).

4.2.7.2. Trace active fat directly surrounding the kidneys, until metabolic activity is no longer present.

4.2.7.3. Adjust abdominal ROIs within this region to exclude the ureters if the SUVmax voxel appears within or near the medial portion of the kidneys.

5. Quality Assurance

5.1. Examine the MIP for any obvious false positives after ROIs have been drawn on all axial slices measured from the C3 vertebrae to around L3-4.

5.2. Ensure that the red SUVmax voxel is in a region that contains BAT, instead of structures such as the ureters, which display similar density values to BAT and very high SUV values.

5.3. Save the final .csv file when certain that all BAT has been identified and all false-positives have been excluded.

6. Segmenting BAT into Individual Depots

Note: The following section is focused only on quantifying regional depots of BAT[17]. The steps are not necessary to obtain whole body BAT volume and activity.

6.1. Generate a BAT mask in the "brown fat, ROI" editor (**Figure 1**).

Note: The mask is defined as a regenerated PET image containing only SUV values for voxels confirmed as BAT within the ROIs created during the previous steps of this protocol. The SUV value for all other voxels is set to 0.

6.1.1. Keep PET/CT Viewer open with all identified BAT or reopen PET/CT Viewer from the "Plug-Ins" drop down menu and load ROIs saved above.

6.1.1.1. Open the three sets of the subject's scan.

6.1.1.2. Open the "brown fat, ROI" dialog box.

6.1.2. Select the "mask" tab and press "Make masked PET".

6.1.3. Wait for an additional box to pop up, with the filename beginning with "DUP_..."

6.1.4. Close the PET/CT Viewer, but leave the individual boxes (with the CT and PET scans) open, and then re-open a new PET/CT Viewer window.

6.1.5. Select the following three checkboxes in the dialog box that appears: the CT set, UPET set, and the latest CPET set (*i.e.,* the CPET set closest to the bottom of the list) - this is the file containing the mask generated earlier.

6.1.6. Change the view of the PET/CT images to sagittal and start drawing all ROIs for region-wide analysis start at the same sagittal slice.

Note: The MIP image orientation will not change. Also, the most central slice (*i.e.,* along the center of the spine) is a good starting location.

6.1.7. Change slice limits to range from slice 1 to the last slice in the scan being analyzed.

6.1.8. Uncheck the density (HU) threshold and change the lower limit of the PET (SUV) threshold to 0.01 SUV to exclude any non-BAT voxels, which now have an SUV value of 0. Check the box above the "Draw Next" button.

6.1.8.1. Label regions by typing the desired label (*e.g.* "cervical", "supraclavicular", *etc.*) into the text field at the bottom left of the "Brown fat, ROI" dialog box.

6.2. Draw and label the cervical ROI (**Figure 3a**) by beginning at the top of C3 and extending the ROI to C7, drawing a line under the body of C7 before closing the ROI.

6.3. Draw and label the supraclavicular ROI (**Figure 3b**).

6.3.1. Begin at C7, but do not include the body of the thoracic vertebrae while extending the ROI to T3, then extend the left border of the ROI to the top of the manubrium of the sternum.

6.3.2. Line the right border of the ROI up with the anterior edge of the body of the thoracic vertebrae included within this region.

6.4. Draw and label the axillary ROI (**Figure 3c**).

6.4.1. Begin at T3, but do not include the body of thoracic vertebrae while extending the ROI to T7, then extend the left border of the ROI short of the body of the sternum.

6.4.2. Line the right border of the ROI with the anterior edge of the body of the thoracic vertebrae included within this region.

6.5. Draw and label the mediastinal ROI (**Figure 3d**) by encompassing the entire sternum within a single ROI.

6.6. Draw and label the Paraspinal ROI (**Figure 3e**) beginning at T1, including all thoracic vertebrae (until T12) within the ROI.

6.6.1. Line the left border of the ROI with the anterior edge of the body of the thoracic vertebrae. Extend the right border of the ROI so that all BAT in the region is included.

6.7. Draw and label the Abdominal ROI (**Figure 3f**) by beginning at the top of L1 and include any BAT that was not accounted for in any of the other previous regions within the abdominal ROI.

6.8. Draw and label the dorsocervical ROI (**Figure 3g**).

6.8.1. Include the region of dorsal subcutaneous fat near the cervical and top of the paraspinal region; this is where the subject's body has made contact with the scanning bed.

6.9. Check "show all" to display the ROIs of all regions to line up all ROIs to prevent overlapping or under-estimation.

6.9.1.1. Position the perimeter of adjacent ROIs flush with each other, so that no BAT is included in two regions, and that no BAT is missing from all regions.

6.9.2. Observe the MIP from both the front and side views to check if all slices are being included in the delineated regions. Check the slice limits if there are areas that are not highlighted in blue (Step 6.2.2).

6.10. Save the final data into a new .csv file. This file will contain regional totals or averages for all BAT parameters from each identified depot.

REPRESENTATIVE RESULTS:

BAT is quantified through a series of post image-acquisition processing steps as shown in **Figure 1**. PET and CT thresholds are used to identify voxels that are metabolically active and have the density of adipose tissue. However, some voxels meeting these criteria can occur in anatomical locations not likely to contain BAT. To avoid these false positives, PET, CT, and anatomical information must all be considered when drawing ROIs (**Figure 2**). Several common regions to include and avoid when quantifying whole body BAT in cold-stimulated subjects are shown in **Figure 2**, such as metabolically active cervical BAT *vs.* salivary glands, vocal chords, and thyroid (**Figures 2A and 2B**); supraclavicular BAT *vs.* shivering muscle near borders of air and solid tissue (*e.g.* intercostal muscles) (**Figure 2C**); and abdominal BAT *vs.* the calyces of the kidneys as they clear labeled glucose (**Figure 2D**). After the ROI's of each axial slice are compiled, BAT depots can be segmented in the sagittal plane to examine intra-/inter-individual differences in regional BAT activation (**Figure 3**).

FIGURE AND TABLE LEGENDS:

Figure 1. Schematic Flow of the Image Processing Steps. First, PET images and corresponding

CT images are uploaded into the PET/CT plug-in (A). After axial ROIs are drawn on each PET/CT slice (B), each voxel meeting both PET and CT criteria are identified in blue (C). A mask is generated from these BAT-identified voxels (D), which is substituted for the original corrected PET scan (E), and depots are segmented in the sagittal view (F).

Figure 2. Axial BAT Region-of-Interest Selection and Common Areas To Avoid in Multiple BAT Depots. Axial slices from a fused PET/CT image (columns 1 and 2) and a maximal intensity projection image (MIP, column 3) with green lines to denote slice height from a scan acquired following cold-stimulation. Green ROIs are drawn around areas with adipose tissue density, high FDG uptake, and anatomical locations likely to contain active BAT in columns 1 and 2. Anatomical areas unlikely to contain BAT are highlighted in red in column 2. Voxels meeting the BAT PET and CT criteria are confirmed by ImageJ and highlighted in blue. Examples are taken from the (A) anterior cervical depot, (B) cervical depot at the level of the thyroid, (C) Supraclavicular/Axillary depot nearby shivering skeletal muscle (*i.e.,* Intercostals), and (D) the Abdominal depot at the level of the ureters of the kidneys.

Figure 3. Regional Segmentation of Seven BAT Depots in the Sagittal View. Following the generation of a "BAT mask" image containing only PET voxels previously identified as active BAT, the following regions can be separated with ROIs drawn in the sagittal plane: (A) Cervical (C3-C7), (B) Supraclavicular (C7-T3, excluding vertebrae), (C) Axillary (T3-T7, excluding vertebrae), (D) Mediastinal (anterior mediastinum), (E) Paraspinal (T1-T12, from the anterior edge of the vertebrae to the spinous processes), (F) Abdominal (T12-L3, retroperitoneal), and (G) Dorsocervical (fat depot distinct and posterior to the paraspinal depot; near the cervical region). The composite image with all regions appears in (H).

DISCUSSION:

Since confirmation of functional BAT in adult humans, there has been great interest in understanding the role of BAT in human physiology. However, because this thermogenic tissue is often found in narrow fascial planes, interspersed within white fat, and surrounding other organs, it is challenging to quantify. In 2016, a consensus document was published by an International BAT expert panel with recommendations for reporting relevant participant characteristics, criteria for subject preparation, and a protocol for acquiring PET/CT images[21]. The panel also identified the need for more consistency in the processing of PET/CT for BAT quantification, noting that methods to identify BAT have varied widely and, in most cases, only limited detail of the BAT quantification procedure is provided. Consequently, while reports of within study reproducibility are high[22–24], appreciably different BAT volume and activity has been reported by groups using different quantification methods, even when participants are of similar age, sex, and BMI[25, 26]. These inconsistencies make comparing findings difficult, and have led to a controversy over the amount of BAT in the adult human[15].

An inherent limitation of PET/CT image processing is the inclusion of voxels that meet both PET and CT criteria but are in anatomical locations that correspond to structures other than BAT. Perfect co-registration of PET and CT images is nearly impossible due to differences in resolution and subject motion during scans. As a consequence, structures bordering air or bone

and regions of high tracer uptake are often incorrectly identified as active BAT. To limit inclusion of false positive voxels, one should apply PET and CT criteria only within the ROIs that users construct. But current approaches to quantify BAT with user-specified ROIs or automated analyses differ in the amount of user involvement and knowledge they require. We have shown that using a single, two-dimensional user-defined coronal ROI applied to the entire stack of images may be more prone to including false positive areas[19]. Several groups have developed automated methods to quantify BAT that are capable of rapidly processing large datasets without much user input. However, these methods either fail to include all potential BAT-containing regions, particularly in the lower body[27], or incur relatively high rates of false positives[28] and false negatives[26]. Since the volume of human BAT is generally low (<600 mL, or <2% of total body mass), small absolute errors in quantification may lead to large relative differences.

The more rigorous approach described by this study of drawing ROIs on each axial PET-CT slice allows the detection of BAT in narrow fascial layers while providing more confidence that false positives have been excluded. This yields a detailed quantification in each individial, rather than a binary assessment of BAT's presence or absence[29]. Therefore, it may be more suitable for controlled experiments in small sample sizes intending to study BAT physiology and/or effects from interventions. Furthermore, the ability to define region-specific BAT depots may provide more insight into BAT's functional relevance and developmental origin. We believe these quantitative measures are important not only for comparison across the field, but also to better estimate BAT's contribution to energy metabolism and thermoregulation in adult humans.

Several anatomical features of BAT will help users of our method limit inclusion of false positive voxels. BAT is typically found in continuous and symmetric fascial layers. Thus, while drawing and refining an ROI, examining the superior and inferior axial slices for continuity and symmetry of the selected adipose tissue can help users maximize inclusion of adipose tissue while minimizing inclusion of skeletal muscle, bone, and other obvious non-BAT structures. Active BAT is also rarely present in subcutaneous adipose depots, so we advise users to avoid these areas when constructing ROIs. As noted in the protocol, BAT is distributed in several distinct anatomical regions, including the cervical, dorsocervical, supraclavicular, axillary, mediastinal, paraspinal, and abdominal depots. These depots are distributed such that one axial slice may contain more than BAT from multiple depots. For instance, an axial slice in the thoracic region can contain BAT from the mediastinal depot (proximal and anterior), paraspinal depot (proximal and posterior, along the spine), and axillary depot (lateral and near the mid-antero-posterior line). Knowledge of these depots can help users create ROIs in the various regions of the body, since they occur in pre-described locations are largely contiguous, as described in our protocol. However, because we encourage users to draw only one ROI per slice to avoid ROI overlap, the additional steps of generating a BAT mask and drawing sagittal ROIs is required to separate the previously-identified BAT voxels into the distinct regional depots if information of BAT distribution is desired, *i.e.,* separating mediastinal, paraspinal, and axillary BAT detected in the same axial ROI into depots based on sagital location (**Figure 3**).

The PET/CT viewer software can also be used to quantify the activity of tissues other than BAT, for instance shivering skeletal muscle, which also major plays a role cold induced thermogenesis[19], or various areas of the brain or liver that have been suggested as reference tissues for PET/CT analysis[21]. However, these tissues will have densities and anatomical distributions that differ from BAT and are outside the focus of our current protocol. We direct readers to the consensus document for greater detail on these subjects[21]. Finally, we advise all users to continually update ImageJ and visit petctviewer.org for Plug-in updates and software assistance.

Though we believe that this rigorous method is more precise than automated methods[26,28] and methods that use a simplified, single ROI to estimate total BAT volume[9, 30], it is not without limitations. There is no ideal method to non-invasively quantify BAT in humans, and ^{18}F-FDG represents only glucose uptake, which is not the same as glucose metabolism[11]. However, even though other radioactive tracers have been used[31–33], ^{18}F-FDG is the most prominent tracer used to study human BAT. Thus, developing standardized methods to analyze ^{18}F-FDG PET/CT images will continue to be impactful in the study of human BAT physiology for the foreseeable future.

The method we propose, creating an ROI on each BAT-containing axial slice while avoiding common problem areas, is labor intensive and requires the user to have some knowledge of underlying anatomy. It is also possible that the stringent ROI selection may introduce false negatives, since some BAT-containing depots may be avoided. Drawing ROIs on every axial slice of the fused PET/CT image allows for careful discrimination between adipose tissue and neighboring metabolically active tissues and/or regions impacted by spill over and partial volume effects[34]. However, the time it takes to complete analysis of a single scan can range from three to eight hours, with the possibility of shortening the time frame with practice and experience. Various machine learning approaches may be able to reduce the labor and expertise required to accomplish this task. However, creating a more automated method that can accurately detect BAT and is robust to false positives created by current imaging limitations will require a large dataset with individuals of varied body composition and BAT distribution. We hope that this method can be used to produce a detailed BAT atlas that may serve as a template for more sophisticated big data approaches.

In conclusion, we demonstrated a step-by-step image analysis approach to quantify human brown adipose tissue volume, activity, and distribution using cold-induced FDG PET/CT scans. The critical steps include 1) continuously and sequentially analyzing axial ROIs and 2) assessing relevant BAT depots by their anatomical location while avoiding other metabolically active tissues. This rigorous quantification approach can be used by investigators in the field to study BAT physiology and serve as reference standard for developing automated human BAT quantitation approaches in the future.

ACKNOWLEDGMENTS:
We would like to thank all of the study volunteers, nursing and clinical staff, and the dieticians of the NIH Clinical Center for their participation in our cold exposure studies and care provided

during the inpatient stays. We'd also like to thank Dr. Bill Dieckmann for all of his assistance with the acquisition and distribution of the PET-CT images for our studies. This work was supported by Intramural Research Program of the National Institute of Diabetes and Digestive and Kidney Diseases Grants Z01 DK071014 (to K.Y.C.) and DK075116-02 (to A.M.C.).

DISCLOSURES:

The authors have nothing to disclose.

REFERENCES:

1. Bovet, P., Chiolero, A., Gedeon, J. Health effects of overweight and obesity in 195 countries. *The New England Journal of Medicine*. **377** (15), 1495–1496, doi: 10.1056/NEJMc1710026 (2017).
2. Maughan, R. Carbohydrate metabolism. *Surgery (Oxford)*. **27** (1), 6–10, doi: 10.1016/j.mpsur.2008.12.002 (2009).
3. Cypess, A.M. *et al.* Identification and importance of brown adipose tissue in adult humans. *The New England Journal of Medicine*. **360** (15), 1509–1517, doi: 10.1056/NEJMoa0810780 (2009).
4. van Marken Lichtenbelt, W.D. *et al.* Cold-activated brown adipose tissue in healthy men. *The New England Journal of Medicine*. **360** (15), 1500–1508, doi: 10.1056/NEJMoa0808718 (2009).
5. Virtanen, K.A. *et al.* Functional brown adipose tissue in healthy adults. *The New England Journal of Medicine*. **360** (15), 1518–1525, doi: 10.1056/NEJMoa0808949 (2009).
6. Abreu-Vieira, G., Xiao, C., Gavrilova, O., Reitman, M.L. Integration of body temperature into the analysis of energy expenditure in the mouse. *Molecular Metabolism*. **4** (6), 461–470, doi: 10.1016/j.molmet.2015.03.001 (2015).
7. Cypess, A.M., Kahn, C.R. Brown fat as a therapy for obesity and diabetes. *Current Opinion in Endocrinology, Diabetes, and Obesity*. **17** (2), 143–149, doi: 10.1097/MED.0b013e328337a81f (2010).
8. Orava, J. *et al.* Different metabolic responses of human brown adipose tissue to activation by cold and insulin. *Cell Metabolism*. **14** (2), 272–279, doi: 10.1016/j.cmet.2011.06.012 (2011).
9. Chen, K.Y. *et al.* Brown fat activation mediates cold-induced thermogenesis in adult humans in response to a mild decrease in ambient temperature. *The Journal of Clinical Endocrinology and Metabolism*. **98** (7), E1218-1223, doi: 10.1210/jc.2012-4213 (2013).
10. Ouellet, V. *et al.* Brown adipose tissue oxidative metabolism contributes to energy expenditure during acute cold exposure in humans. *The Journal of Clinical Investigation*. **122** (2), 545–552, doi: 10.1172/JCI60433 (2012).
11. Blondin, D.P. *et al.* Contributions of white and brown adipose tissues and skeletal muscles to acute cold-induced metabolic responses in healthy men. *The Journal of Physiology*. **593** (3), 701–714, doi: 10.1113/jphysiol.2014.283598 (2015).
12. Ruiz, J.R., Martinez-Tellez, B., Sanchez-Delgado, G., Aguilera, C.M., Gil, A. Regulation of energy balance by brown adipose tissue: at least three potential roles for physical activity. *British Journal of Sports Medicine*. **49** (15), 972–973, doi: 10.1136/bjsports-2014-094537 (2015).
13. Bakker, L.E.H. *et al.* Brown adipose tissue volume in healthy lean south Asian adults compared with white Caucasians: a prospective, case-controlled observational study. *The Lancet Diabetes & Endocrinology*. **2** (3), 210–217, doi: 10.1016/S2213-8587(13)70156-6 (2014).
14. Lee, P. *et al.* Temperature-acclimated brown adipose tissue modulates insulin sensitivity in

humans. *Diabetes*. **63** (11), 3686–3698, doi: 10.2337/db14-0513 (2014).
15. Jensen, M.D. Brown adipose tissue – not as hot as we thought. *The Journal of Physiology*. **593** (3), 489–490, doi: 10.1113/jphysiol.2014.287979 (2015).
16. Heaton, J.M. The distribution of brown adipose tissue in the human. *Journal of Anatomy*. **112** (Pt 1), 35–39 (1972).
17. Chauvie, S., Bertone, E., Bergesio, F., Terulla, A., Botto, D., Cerello, P. Automatic liver detection and standardised uptake value evaluation in whole-body Positron Emission Tomography/Computed Tomography scans. *Computer Methods and Programs in Biomedicine*. **156**, 47–52, doi: 10.1016/j.cmpb.2017.12.026 (2018).
18. Chondronikola, M., Beeman, S.C., Wahl, R.L. Non-invasive methods for the assessment of brown adipose tissue in humans. *The Journal of Physiology*. **596** (3), 363–378, doi: 10.1113/JP274255 (2018).
19. Leitner, B.P. *et al.* Mapping of human brown adipose tissue in lean and obese young men. *Proceedings of the National Academy of Sciences of the United States of America*. **114** (32), 8649–8654, doi: 10.1073/pnas.1705287114 (2017).
20. Martinez-Tellez, B. *et al.* The impact of using BARCIST 1.0 criteria on quantification of BAT volume and activity in three independent cohorts of adults. *Scientific Reports*. **8** (1), 8567, doi: 10.1038/s41598-018-26878-4 (2018).
21. Chen, K.Y. *et al.* Brown Adipose Reporting Criteria in Imaging STudies (BARCIST 1.0): recommendations for standardized FDG-PET/CT experiments in humans. *Cell Metabolism*. **24** (2), 210–222, doi: 10.1016/j.cmet.2016.07.014 (2016).
22. Rasmussen, J.M. *et al.* Brown adipose tissue quantification in human neonates using water-fat separated MRI. *PloS One*. **8** (10), e77907, doi: 10.1371/journal.pone.0077907 (2013).
23. Becker, A.S. *et al.* In-depth analysis of interreader agreement and accuracy in categorical assessment of brown adipose tissue in (18)FDG-PET/CT. *European Journal of Radiology*. **91**, 41–46, doi: 10.1016/j.ejrad.2017.03.012 (2017).
24. Lee, Y.-H., Hsiao, H.-F., Yang, H.-T., Huang, S.-Y., Chan, W.P. Reproducibility and repeatability of computer tomography-based measurement of abdominal subcutaneous and visceral adipose tissues. *Scientific Reports*. **7**, 40389, doi: 10.1038/srep40389 (2017).
25. Lundström, E., Strand, R., Johansson, L., Bergsten, P., Ahlström, H., Kullberg, J. Magnetic resonance imaging cooling-reheating protocol indicates decreased fat fraction via lipid consumption in suspected brown adipose tissue. *PLOS One*. **10** (4), e0126705, doi: 10.1371/journal.pone.0126705 (2015).
26. Gifford, A., Towse, T.F., Walker, R.C., Avison, M.J., Welch, E.B. Human brown adipose tissue depots automatically segmented by positron emission tomography/computed tomography and registered magnetic resonance images. *Journal of Visualized Experiments*. (96), doi: 10.3791/52415 (2015).
27. Jones, T.A. *et al.* Brown fat depots in adult humans remain static in their locations on PET/CT despite changes in seasonality. *Physiological Reports*. **5** (11), doi: 10.14814/phy2.13284 (2017).
28. Ruth, M.R., Wellman, T., Mercier, G., Szabo, T., Apovian, C.M. An automated algorithm to identify and quantify brown adipose tissue in human 18F-FDG-PET/CT scans. *Obesity (Silver Spring, Md.)*. **21** (8), 1554–1560, doi: 10.1002/oby.20315 (2013).
29. Hibi, M. *et al.* Brown adipose tissue is involved in diet-induced thermogenesis and whole-

body fat utilization in healthy humans. *International Journal of Obesity (2005)*. **40** (11), 1655–1661, doi: 10.1038/ijo.2016.124 (2016).
30. Hanssen, M.J.W. *et al.* Short-term cold acclimation recruits brown adipose tissue in obese humans. *Diabetes*. **65** (5), 1179–1189, doi: 10.2337/db15-1372 (2016).
31. Muzik, O., Mangner, T.J., Leonard, W.R., Kumar, A., Janisse, J., Granneman, J.G. 15O PET measurement of blood flow and oxygen consumption in cold-activated human brown fat. *Journal of Nuclear Medicine: Official Publication, Society of Nuclear Medicine*. **54** (4), 523–531, doi: 10.2967/jnumed.112.111336 (2013).
32. Blondin, D.P. *et al.* Inhibition of intracellular triglyceride lipolysis suppresses cold-induced brown adipose tissue metabolism and increases shivering in humans. *Cell Metabolism*. **25** (2), 438–447, doi: 10.1016/j.cmet.2016.12.005 (2017).
33. Admiraal, W.M., Holleman, F., Bahler, L., Soeters, M.R., Hoekstra, J.B., Verberne, H.J. Combining 123I-metaiodobenzylguanidine SPECT/CT and 18F-FDG PET/CT for the assessment of brown adipose tissue activity in humans during cold exposure. *Journal of Nuclear Medicine: Official Publication, Society of Nuclear Medicine*. **54** (2), 208–212, doi: 10.2967/jnumed.112.111849 (2013).
34. Soret, M., Bacharach, S.L., Buvat, I. Partial-volume effect in PET tumor imaging. *Journal of Nuclear Medicine: Official Publication, Society of Nuclear Medicine*. **48** (6), 932–945, doi: 10.2967/jnumed.106.035774 (2007).

Figure 01

Click here to download Figure JoVE Figure1_07.09.18.pdf

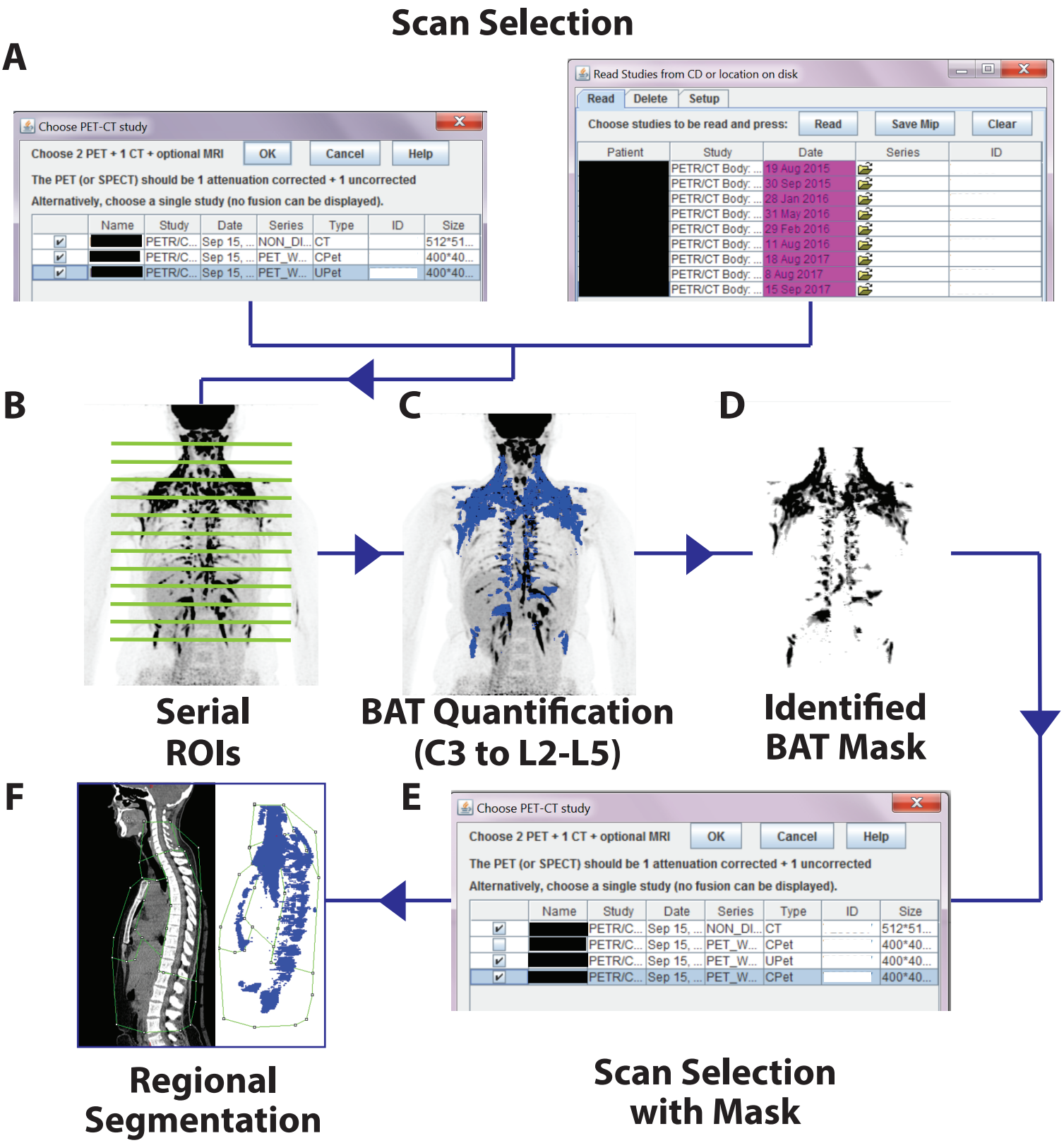

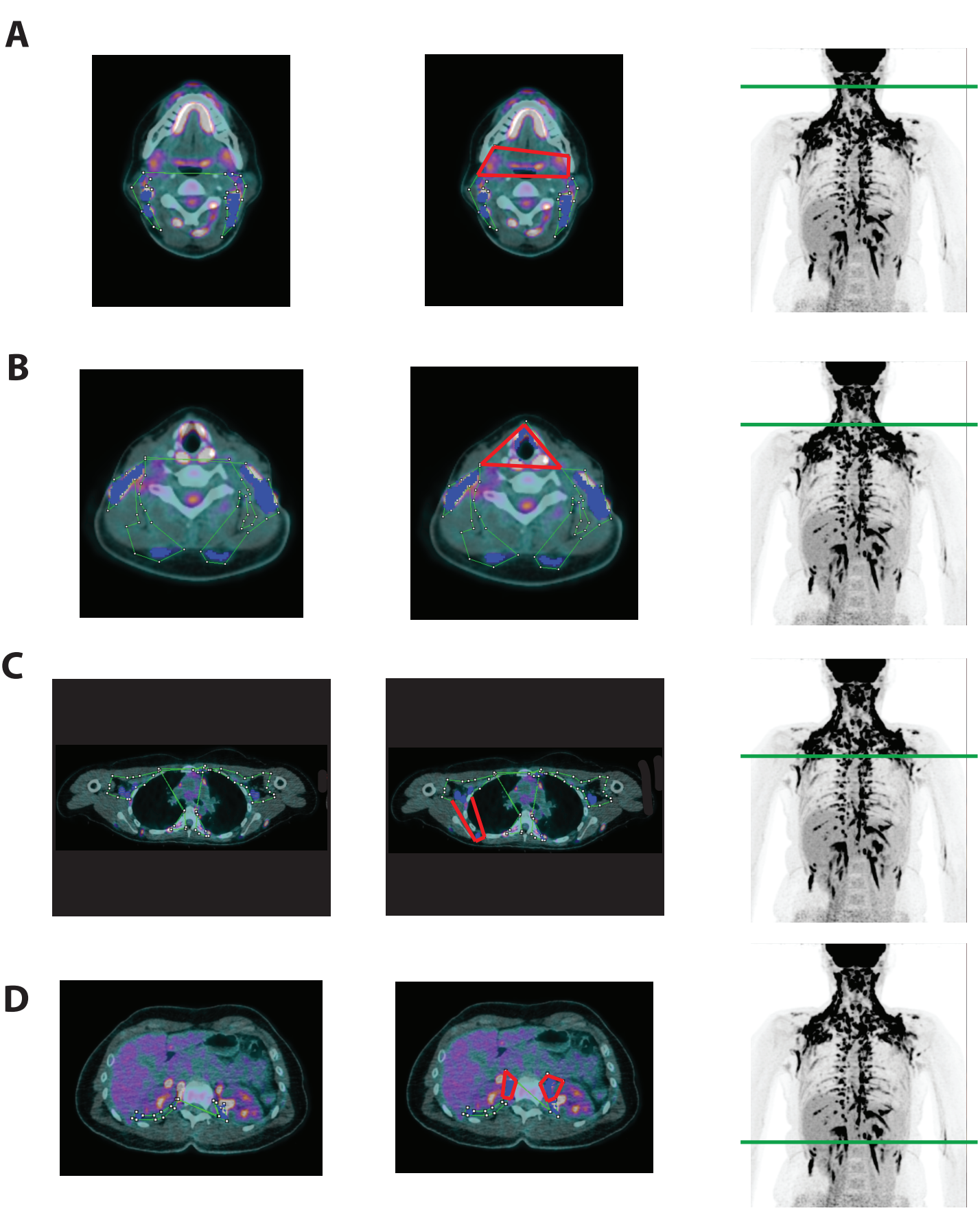

A

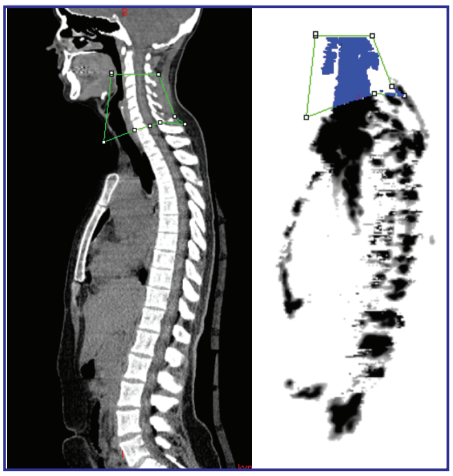

Cervical

B

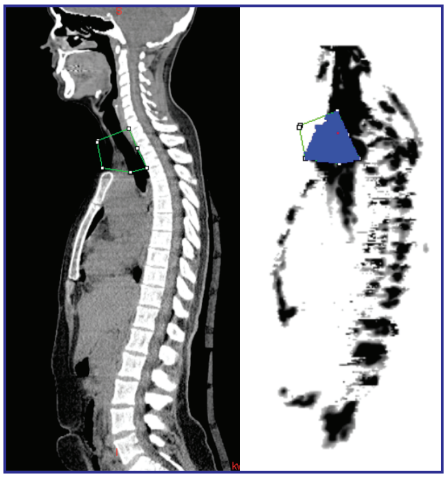

Supraclavicular

C

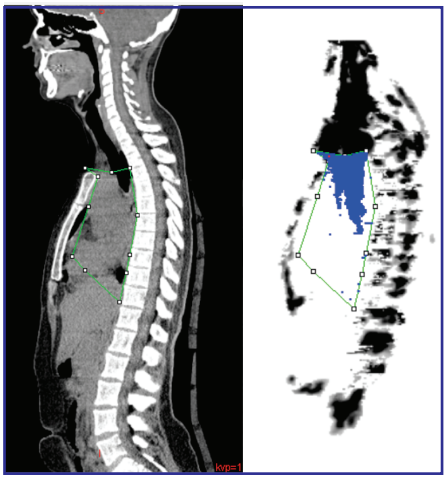

Axillary

D

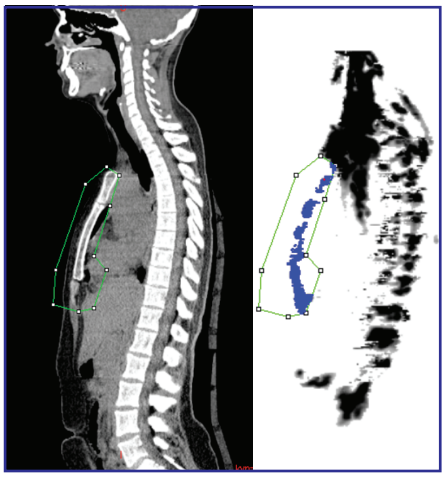

Mediastinal

E

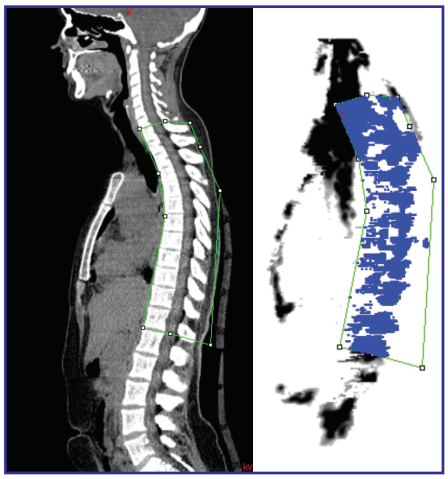

Paraspinal

F

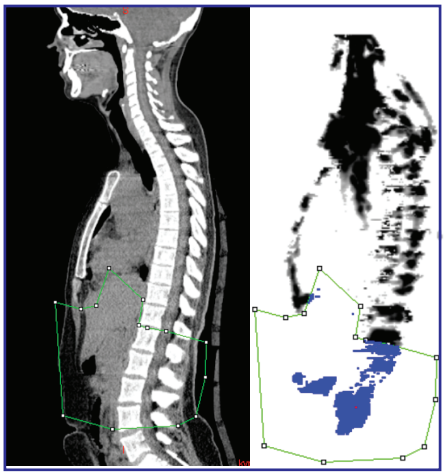

Abdominal

G

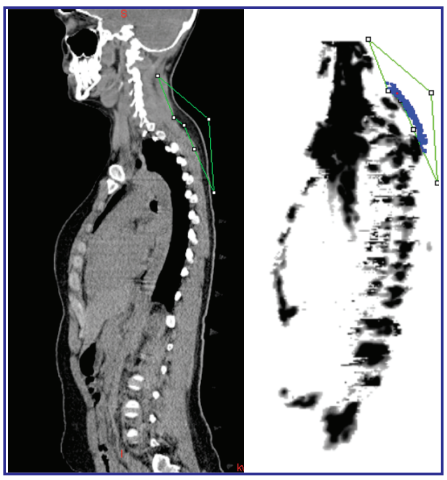

Dorsocervical

H

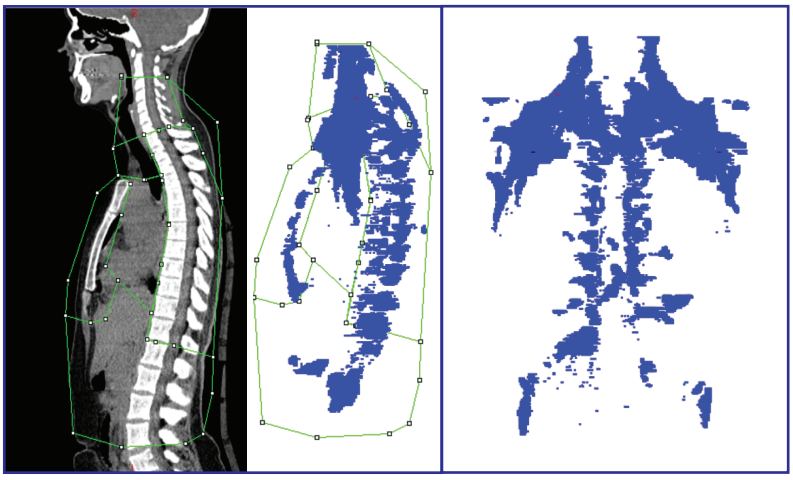

All Regions (Sagittal)

(Frontal)

Materials Table

Click here to download Table of Materials JoVE_Materials.xls

Name of Material/ Equipment	Company	Catalog Number	Comments/Description
ImageJ/Fiji Software	ImageJ	https://imagej.net/Fiji/Downloads	Open Source Software

jove JOURNAL OF VISUALIZED EXPERIMENTS
1 Alewife Center #200
Cambridge, MA 02140
tel. 617.945.9051
www.jove.com

ARTICLE AND VIDEO LICENSE AGREEMENT

Title of Article: Whole Body and Regional Quantification of Active Human Brown Adipose Tissue Using ^{18}F-FDG PET/CT

Author(s): Kim, K, Huang, S, Fletcher, LA, O'Mara, AE, Tal, I, Brychta, RJ, Cypess, AM, Chen, KY, Leitner, BP

Item 1 (check one box): The Author elects to have the Materials be made available (as described at http://www.jove.com/author) via: [ ] Standard Access [X] Open Access

Item 2 (check one box):

[ ] The Author is NOT a United States government employee.

[X] The Author is a United States government employee and the Materials were prepared in the course of his or her duties as a United States government employee.

[ ] The Author is a United States government employee but the Materials were NOT prepared in the course of his or her duties as a United States government employee.

ARTICLE AND VIDEO LICENSE AGREEMENT

1. Defined Terms. As used in this Article and Video License Agreement, the following terms shall have the following meanings: "**Agreement**" means this Article and Video License Agreement; "**Article**" means the article specified on the last page of this Agreement, including any associated materials such as texts, figures, tables, artwork, abstracts, or summaries contained therein; "**Author**" means the author who is a signatory to this Agreement; "**Collective Work**" means a work, such as a periodical issue, anthology or encyclopedia, in which the Materials in their entirety in unmodified form, along with a number of other contributions, constituting separate and independent works in themselves, are assembled into a collective whole; "**CRC License**" means the Creative Commons Attribution-Non Commercial-No Derivs 3.0 Unported Agreement, the terms and conditions of which can be found at: http://creativecommons.org/licenses/by-nc-nd/3.0/legalcode; "**Derivative Work**" means a work based upon the Materials or upon the Materials and other pre-existing works, such as a translation, musical arrangement, dramatization, fictionalization, motion picture version, sound recording, art reproduction, abridgment, condensation, or any other form in which the Materials may be recast, transformed, or adapted; "**Institution**" means the institution, listed on the last page of this Agreement, by which the Author was employed at the time of the creation of the Materials; "**JoVE**" means MyJove Corporation, a Massachusetts corporation and the publisher of *The Journal of Visualized Experiments;* "**Materials**" means the Article and / or the Video; "**Parties**" means the Author and JoVE; "**Video**" means any video(s) made by the Author, alone or in conjunction with any other parties, or by JoVE or its affiliates or agents, individually or in collaboration with the Author or any other parties, incorporating all or any portion of the Article, and in which the Author may or may not appear.

2. Background. The Author, who is the author of the Article, in order to ensure the dissemination and protection of the Article, desires to have the JoVE publish the Article and create and transmit videos based on the Article. In furtherance of such goals, the Parties desire to memorialize in this Agreement the respective rights of each Party in and to the Article and the Video.

3. Grant of Rights in Article. In consideration of JoVE agreeing to publish the Article, the Author hereby grants to JoVE, subject to **Sections 4** and **7** below, the exclusive, royalty-free, perpetual (for the full term of copyright in the Article, including any extensions thereto) license (a) to publish, reproduce, distribute, display and store the Article in all forms, formats and media whether now known or hereafter developed (including without limitation in print, digital and electronic form) throughout the world, (b) to translate the Article into other languages, create adaptations, summaries or extracts of the Article or other Derivative Works (including, without limitation, the Video) or Collective Works based on all or any portion of the Article and exercise all of the rights set forth in (a) above in such translations, adaptations, summaries, extracts, Derivative Works or Collective Works and (c) to license others to do any or all of the above. The foregoing rights may be exercised in all media and formats, whether now known or hereafter devised, and include the right to make such modifications as are technically necessary to exercise the rights in other media and formats. If the "Open Access" box has been checked in **Item 1** above, JoVE and the Author hereby grant to the public all such rights in the Article as provided in, but subject to all limitations and requirements set forth in, the CRC License.

4. Retention of Rights in Article. Notwithstanding the exclusive license granted to JoVE in **Section 3** above, the Author shall, with respect to the Article, retain the non-exclusive right to use all or part of the Article for the non-commercial purpose of giving lectures, presentations or teaching classes, and to post a copy of the Article on the Institution's website or the Author's personal website, in each case provided that a link to the Article on the JoVE website is provided and notice of JoVE's copyright in the Article is included. All non-copyright intellectual property rights in and to the Article, such as patent rights, shall remain with the Author.

5. Grant of Rights in Video – Standard Access. This **Section 5** applies if the "Standard Access" box has been checked in **Item 1** above or if no box has been checked in **Item 1** above. In consideration of JoVE agreeing to produce, display or otherwise assist with the Video, the Author hereby acknowledges and agrees that, Subject to **Section 7** below, JoVE is and shall be the sole and exclusive owner of all rights of any nature, including, without limitation, all copyrights, in and to the Video. To the extent that, by law, the Author is deemed, now or at any time in the future, to have any rights of any nature in or to the Video, the Author hereby disclaims all such rights and transfers all such rights to JoVE.

6. Grant of Rights in Video – Open Access. This **Section 6** applies only if the "Open Access" box has been checked in **Item 1** above. In consideration of JoVE agreeing to produce, display or otherwise assist with the Video, the Author hereby grants to JoVE, subject to **Section 7** below, the exclusive, royalty-free, perpetual (for the full term of copyright in the Article, including any extensions thereto) license (a) to publish, reproduce, distribute, display and store the Video in all forms, formats and media whether now known or hereafter developed (including without limitation in print, digital and electronic form) throughout the world, (b) to translate the Video into other languages, create adaptations, summaries or extracts of the Video or other Derivative Works or Collective Works based on all or any portion of the Video and exercise all of the rights set forth in (a) above in such translations, adaptations, summaries, extracts, Derivative Works or Collective Works and (c) to license others to do any or all of the above. The foregoing rights may be exercised in all media and formats, whether now known or hereafter devised, and include the right to make such modifications as are technically necessary to exercise the rights in other media and formats. For any Video to which this Section 6 is applicable, JoVE and the Author hereby grant to the public all such rights in the Video as provided in, but subject to all limitations and requirements set forth in, the CRC License.

7. Government Employees. If the Author is a United States government employee and the Article was prepared in the course of his or her duties as a United States government employee, as indicated in **Item 2** above, and any of the licenses or grants granted by the Author hereunder exceed the scope of the 17 U.S.C. 403, then the rights granted hereunder shall be limited to the maximum rights permitted under such statute. In such case, all provisions contained herein that are not in conflict with such statute shall remain in full force and effect, and all provisions contained herein that do so conflict shall be deemed to be amended so as to provide to JoVE the maximum rights permissible within such statute.

8. Likeness, Privacy, Personality. The Author hereby grants JoVE the right to use the Author's name, voice, likeness, picture, photograph, image, biography and performance in any way, commercial or otherwise, in connection with the Materials and the sale, promotion and distribution thereof. The Author hereby waives any and all rights he or she may have, relating to his or her appearance in the Video or otherwise relating to the Materials, under all applicable privacy, likeness, personality or similar laws.

9. Author Warranties. The Author represents and warrants that the Article is original, that it has not been published, that the copyright interest is owned by the Author (or, if more than one author is listed at the beginning of this Agreement, by such authors collectively) and has not been assigned, licensed, or otherwise transferred to any other party. The Author represents and warrants that the author(s) listed at the top of this Agreement are the only authors of the Materials. If more than one author is listed at the top of this Agreement and if any such author has not entered into a separate Article and Video License Agreement with JoVE relating to the Materials, the Author represents and warrants that the Author has been authorized by each of the other such authors to execute this Agreement on his or her behalf and to bind him or her with respect to the terms of this Agreement as if each of them had been a party hereto as an Author. The Author warrants that the use, reproduction, distribution, public or private performance or display, and/or modification of all or any portion of the Materials does not and will not violate, infringe and/or misappropriate the patent, trademark, intellectual property or other rights of any third party. The Author represents and warrants that it has and will continue to comply with all government, institutional and other regulations, including, without limitation all institutional, laboratory, hospital, ethical, human and animal treatment, privacy, and all other rules, regulations, laws, procedures or guidelines, applicable to the Materials, and that all research involving human and animal subjects has been approved by the Author's relevant institutional review board.

10. JoVE Discretion. If the Author requests the assistance of JoVE in producing the Video in the Author's facility, the Author shall ensure that the presence of JoVE employees, agents or independent contractors is in accordance with the relevant regulations of the Author's institution. If more than one author is listed at the beginning of this Agreement, JoVE may, in its sole discretion, elect not take any action with respect to the Article until such time as it has received complete, executed Article and Video License Agreements from each such author. JoVE reserves the right, in its absolute and sole discretion and without giving any reason therefore, to accept or decline any work submitted to JoVE. JoVE and its employees, agents and independent contractors shall have

jove JOURNAL OF VISUALIZED EXPERIMENTS
1 Alewife Center #200
Cambridge, MA 02140
tel. 617.945.9051
www.jove.com

ARTICLE AND VIDEO LICENSE AGREEMENT

full, unfettered access to the facilities of the Author or of the Author's institution as necessary to make the Video, whether actually published or not. JoVE has sole discretion as to the method of making and publishing the Materials, including, without limitation, to all decisions regarding editing, lighting, filming, timing of publication, if any, length, quality, content and the like.

11. Indemnification. The Author agrees to indemnify JoVE and/or its successors and assigns from and against any and all claims, costs, and expenses, including attorney's fees, arising out of any breach of any warranty or other representations contained herein. The Author further agrees to indemnify and hold harmless JoVE from and against any and all claims, costs, and expenses, including attorney's fees, resulting from the breach by the Author of any representation or warranty contained herein or from allegations or instances of violation of intellectual property rights, damage to the Author's or the Author's institution's facilities, fraud, libel, defamation, research, equipment, experiments, property damage, personal injury, violations of institutional, laboratory, hospital, ethical, human and animal treatment, privacy or other rules, regulations, laws, procedures or guidelines, liabilities and other losses or damages related in any way to the submission of work to JoVE, making of videos by JoVE, or publication in *JoVE* or elsewhere by JoVE. The Author shall be responsible for, and shall hold JoVE harmless from, damages caused by lack of sterilization, lack of cleanliness or by contamination due to the making of a video by JoVE its employees, agents or independent contractors. All sterilization, cleanliness or decontamination procedures shall be solely the responsibility of the Author and shall be undertaken at the Author's expense. All indemnifications provided herein shall include JoVE's attorney's fees and costs related to said losses or damages. Such indemnification and holding harmless shall include such losses or damages incurred by, or in connection with, acts or omissions of JoVE, its employees, agents or independent contractors.

12. Fees. To cover the cost incurred for publication, JoVE must receive payment before production and publication the Materials. Payment is due in 21 days of invoice. Should the Materials not be published due to an editorial or production decision, these funds will be returned to the Author. Withdrawal by the Author of any submitted Materials after final peer review approval will result in a US$1,200 fee to cover pre-production expenses incurred by JoVE. If payment is not received by the completion of filming, production and publication of the Materials will be suspended until payment is received.

13. Transfer, Governing Law. This Agreement may be assigned by JoVE and shall inure to the benefits of any of JoVE's successors and assignees. This Agreement shall be governed and construed by the internal laws of the Commonwealth of Massachusetts without giving effect to any conflict of law provision thereunder. This Agreement may be executed in counterparts, each of which shall be deemed an original, but all of which together shall be deemed to me one and the same agreement. A signed copy of this Agreement delivered by facsimile, e-mail or other means of electronic transmission shall be deemed to have the same legal effect as delivery of an original signed copy of this Agreement.

A signed copy of this document must be sent with all new submissions. Only one Agreement required per submission.

CORRESPONDING AUTHOR:

Name:	Brooks P. Leitner
Department:	Diabetes, Endocrinology, and Obesity Branch, NIDDK
Institution:	National Institutes of Health
Article Title:	Whole Body and Regional Quantification of Active Human Brown Adipose Tissue Using 18F-FDG PET/CT
Signature:	 Date: 4/26/18

Please submit a signed and dated copy of this license by one of the following three methods:

1) Upload a scanned copy of the document as a pfd on the JoVE submission site;
2) Fax the document to +1.866.381.2236;
3) Mail the document to JoVE / Attn: JoVE Editorial / 1 Alewife Center #200 / Cambridge, MA 02139

For questions, please email submissions@jove.com or call +1.617.945.9051

July 9th, 2018

Rebuttal Letter for JOVE Manuscript "Whole Body and Regional Quantification of Active Human Brown Adipose Tissue Using 18F-FDG PET/CT"

EDITORIAL COMMENTS

1. Please take this opportunity to thoroughly proofread the manuscript to ensure tha t there are no spelling or grammar issues.
   Thank you for the suggestion. We have made careful edits throughout the manuscript.

2. Please provide an email address for each author.
   All emails have now been added.

3. Please rephrase the Introduction to include a clear statement of the overall goal o f this method.
   Thank you for the suggestion. We have now revised this section to enhance focus of the introduction.

4. 3.1 (3.1.1-3.1.3), 3.2 (3.2.1-3.2.3), 3.3, 3.4.1-
   .4.2, 3.6.1, 3.7, 3.7.1, 3.7.2, 3.8.1.2, 3.9.1, 4.1, 4.2, etc: Please revise the protoco l so that all text in the protocol section is written in the imperative tense as if tellin g someone how to do the technique (e.g., "Do this," "Ensure that," etc.). The actio ns should be described in the imperative tense in complete sentences wherever possible. Avoid usage of phrases such as "could be," "should be," and "would be" throughout the Protocol. Any text that cannot be written in the imperative tense may be added as a "Note." However, notes should be concise and used sparingl y. Please move the discussion about the protocol to the Discussion.
   The protocol has been adjusted accordingly. The paragraph originally in the introduction that discussed limitations of other methods has also been moved to the Discussion.

5. For critical computational steps, it would be helpful if software screenshots are pr ovided as supplementary files to match each step.
   We believe that the most critical steps have been highlighted in the current set of figures.

6. There is a 2.75 page limit for filmable content. Please highlight 2.75 pages or les s of the Protocol (including headings and spacing) that identifies the essential ste ps of the protocol for the video, i.e., the steps that should be visualized to tell the most cohesive story of the Protocol. Remember that non-
   highlighted Protocol steps will remain in the manuscript, and therefore will still be

available to the reader.
We have reduced the highlighted text from just over 3.0 pages to about 2.75 pages.

7. Please ensure that the highlighted steps form a cohesive narrative with a logical f low from one highlighted step to the next. Please highlight complete sentences (n ot parts of sentences). Please ensure that the highlighted part of the step include s at least one action that is written in imperative tense. Please do not highlight an y steps describing euthanasia.
Revised as recommended.

8. Please include all relevant details that are required to perform the step in the hi ghlighting. For example: If step 2.5 is highlighted for filming and the details of ho w to perform the step are given in steps 2.5.1 and 2.5.2, then the sub-steps where the details are provided must be highlighted.
Revised as recommended with detail in multiple steps.

9. Please combine some of the shorter Protocol steps so that individual steps co ntain 2-3 actions and maximum of 4 sentences per step.
Revised as recommended. We chose to keep some shorter steps to keep the protocol succinct. We believe these steps will make more sense for the video.

10. Discussion: Please also discuss critical steps within the protocol.
We have added more information about several critical steps in the protocol as suggested.

REVIEWER 1 COMMENTS

Major Concerns:

INTRODUCTION:
In general terms the introduction lacks of key references and the authors do some assumptions that need to be cited.
We now added some key references to address these concerns.

PROTOCOL

1. It will be helpful to prepare a tutorial/video recording of the screen analysing BAT of one participant. This video could be really helpful for the scientific community.

We thank the reviewer for this comment, and we agree that a video version will complement the written instructions of this manuscript, which is the unique approach of this journal. If the paper is accepted, the JoVE staff will provide professional assistance to produce such a video.

2. In the point that stablished in the protocol section, it is mentioned that you used the option of "Any". However, if you read the instruction of the authors you will find the following sentences:

"Even though in most cases the CT has many more points than the corresponding PET point, only nearest neighbours are used. The "best" choice would be average since that would be expected to be fairly close to the central point. The all choice would be more stringent in that all nearest neighbours would have to be in the fat window. Any is the least stringent as even a single CT point in the fat window would accept the PET point."

Based on that argument, the creator of the software stablished (also co-author of this paper), stablished that the best option will be to use "average" instead of "any" or "all". Justify, why you have selected "any".
-Do you have any sensitivity analysis of that?
-How can affect the use of "any" or "all" to the analyses?

If not, I will suggest to replace and re-do it the set of the results based on the average option instead of use any.

We agree that the option to select Any/Average/All will lead to different results of BAT volume and activity. However, the main objectives of this manuscript are primarily to instruct the readers how to construct the axial ROI's and navigate through the image analysis software. While we include the description of each of these options, we prefer to leave this choice to the user depending on their specific research goals. We have modified the text as follows: "Select one of the three voxel inclusion criteria ("Any", "Average", or "All"). NOTE: "Any" was used in Leitner et al. 2017. For a detailed explanation of other options, refer to petctviewer.org"

3. Why do you select the range of -300 to -10, when recently a panel of experts (some of the co-authors of this work) proposed -190 to -10?

We thank the reviewer for this detailed observation. We selected the range of -300 to -10 to be consistent with our last publication using this method (Leitner et al 2017). We have added a clarification to suggest that the user can use the HU range recommended by BARCIST. The text now reads: "NOTE: a -300 HU lower limit and -10 HU upper limit were used in Leitner et al. 2017 and a range from -190 to -10 was also previously recommended (Chen et al 2016)"

4. I will add a section to "Load" the ROIs that were previously drawn.
Revised as recommended in step 2.2. Thank you.

5. Based on the BARCIST 1.0 paper, I will add a section named "Reference tissues" and I will show what is (in your opinion) the best way to draw the ROI in cerebellum, liver and descending aorta as reference tissues.

Thank you for this comment. BARCIST 1.0 is only a recommendation guideline, and there is ongoing debate as to which tissue should be used as reference tissue. The focus of this manuscript is on quantifying human BAT, and thus we do not include the steps to quantifying other tissues. However, we have added the following statement to the discussion to inform readers about analysis of reference tissues: "The PETCT viewer software can also be used to quantify the activity of tissues other than BAT, for instance shivering skeletal muscle which also major plays a role in cold induced thermogenesis (Leitner et al 2017), or various areas of the brain or liver which have been suggested as reference tissues for PET/CT analysis (Chen et al 2016). However, these tissues will have densities and anatomical distributions that differ from BAT and are outside the focus of our current protocol. We direct readers to the consensus document for greater detail on these subjects (Chen et al 2016)."

6. Why the cervical region is stablished from C3 to C7 instead of atlas vertebrae to C7? C1 and C2 you can also find cervical BAT.
It is possible to find cervical BAT near C1 and C2 vertebrae, however these regions are close to the base of the skull and the jaw, where spillover from brain FDG uptake and skeletal muscle uptake may be problematic. We believe that starting at C3 as the vertebral landmark may be the easiest way to standardize BAT quantification across subjects and across researchers. We have clarified this in the revision. The note for this section now reads: "NOTE: C1-C2 regions may also contain BAT, but BAT detection there is likely to be confounded by high uptake of FDG in brain and skeletal muscle."

7. Which are the problematic zones that should be excluded? Please clarify.
Thank you, we believe this is quite an important concept to be made clear through the use of the video which will include these problematic zones in each of the BAT regions. We believe that the screenshots captured in our figures highlight the most common problematic zones as examples.

8. In the paper of Leitner et al. 2017 you also measured skeletal muscle activity. Which skeletal muscles have you measured? Maybe, add this section to this protocol?
Thank you again for this comment. As stated previously, because the focus of this manuscript is on how to quantify active BAT, we have not included a section on how to measure skeletal muscle activity. However, we have added the following statement to the discussion section to inform readers that it is possible

to do this using the software: "The PETCT viewer software can also be used to quantify the activity of tissues other than BAT, for instance shivering skeletal muscle which also major plays a role cold induced thermogenesis (Leitner et al 2017), or various areas of the brain or liver which have been suggested as reference tissues for PET/CT analysis (Chen et al 2016). However, these tissues will have densities and anatomical distributions that differ from BAT and are outside the focus of our current protocol. We direct readers to the consensus document for greater detail on these subjects (Chen et al 2016)."

9. During the description of the protocol, I will add a short intro before starting every point. For instance 6. Segmenting BAT into individuals Depots. I will describe shortly which is the aim to do that and why is better to analyse BAT from the mask instead of analysed BAT directly from the original data.

Thank you for the suggestion. However, due to the strict limitation of space and the format dictated by the journal (see editors comments) we are unable to put a short description before every point in the protocol section. However, for the section that you have mentioned, we added a clarifying note to the beginning of the section and we added further discussion of the segmentation to the discussion. The note now reads: "NOTE: The following section is focused only on quantifying regional depots of BAT[17]. The steps are not necessary to obtain whole body BAT volume and activity."

The portion added to the discussion is also in reference to your next question (#10) and the new text can be found there.

10. Which is the main aim to perform a mask? Is it really needed for human BAT quantification?

We apologize to the reviewer that this part of the manuscript was not clearer. The mask is not required to obtain whole-body BAT volume and activity, it is only required to quantify BAT in regional depots, as noted in our response to your previous question (#9). BAT from multiple regional depots can occur in each axial slice. The PETCT Viewer software only allows the user to draw ROIs in one plane at a time. We chose to perform the axial slice-by-slice analysis first to identify all active BAT throughout the body. The mask is a re-generated PET image where only voxels identified as BAT retain their SUV value. The SUV value for all other voxels is set to 0. Once generated, the user can create ROIs on the mask in the sagittal plane, rather than the axial plane, which is much easier to separate the seven specific depots that we have previously defined, as seen in Figure 3 (new figure numbering).

To address this, we have added several clarifying passages to the text. To section 6 in the protocol, we have added the following: " NOTE: The following section is

focused only on quantifying regional depots of BAT17. The steps are not necessary to obtain whole body BAT volume and activity. Generate a BAT mask in the "brown fat, ROI" editor (Figure 1). NOTE: The mask is a PET image containing SUV values only for voxels identified as BAT with the ROIs created during the previous steps of this protocol. The SUV value for all other voxels is set to 0."

And to the discussion we have added: "As noted in the protocol, BAT is distributed in several distinct anatomical regions, including the cervical, dorsocervical, supraclavicular, axillary, mediastinal, paraspinal, and abdominal depots. These depots are distributed such that one axial slice may contain more than BAT from multiple depots. For instance, an axial slice in the thoracic region can contain BAT from the mediastinal depot (proximal and anterior), paraspinal depot (proximal and posterior, along the spine), and axillary depot (lateral and near the mid-antero-posterior line). Knowledge of these depots can help users create ROIs in the various regions of the body since they occur in pre-described locations are largely contiguous, as described in our protocol. However, because we encourage users to draw only one ROI per slice to avoid ROI overlap, the additional steps of generating a BAT mask and drawing sagittal ROIs is required to separate the previously-identified BAT voxels into the distinct regional depots if information of BAT distribution is desired, i.e. separating mediastinal, paraspinal, and axillary BAT detected in the same axial ROI into depots based on sagital location as shown in Figure 3."

We also hope that the "chapters" available in the video format of this article will also make this section more clear for readers and users.

11. I have followed all the protocol and I did not have any problem to do every step. However, from the 6.2 to 6.10 I have not been able to do it and I do not understand the logic behind. Please explain these steps a little bit better.
As mentioned in the previous comment from the reviewer, we hope that our revisions help clarify the steps in mapping BAT in different depots.

12. Although the proposed method is able to reduce the number false positive cases, it should be considered that it might increase the false negatives, since some specific containing-BAT depots might be avoided (e.g. see Figure 1C, in which paravertebral and pericardial BAT depots seem not to be included within the ROIs).
This is an excellent point.

We have included a note in the discussion to state: "It is also possible that the stringent ROI selection may introduce false negatives since some BAT-containing depots may not be included."

RESULTS

1. Several studies (see PMID: 25384777 and 23362317) have addressed that there are several skeletal muscles such as longuis colli, scalene or sternocleidomastoid which can be confused with cervical BAT in a cold exposure. Nowadays, there is a huge gap in literature about how skeletal muscle glucose uptake is quantified (e.g. anatomical delimitation, slice height, applied SUV and HU range), it might be useful for future studies adding to this extensive protocol a section related to this issue.

We agree that skeletal muscle can play a role in thermogenesis, thus our BAT ROI's try to stay away from skeletal muscles as mentioned by the reviewer. But as stated previously, the purpose of this article focuses on BAT quantification so we chose not to divert our focus to other tissues. However, as stated in our response to question #8 in the protocol section, we have added some text to the discussion section for readers with possible interest in muscle activity.

o Please, explain how to exclude these muscles

In our figures, we show ROIs that try to avoid including muscle groups that tend to experience shivering. We hope to demonstrate these approaches in the video version.

o Which skeletal muscles would you measure or have you measured in Leitner et al. 2017? I will report how to draw a ROI for these skeletal muscles, because in Leitner et al. 2017 you published glucose uptake of this tissue.

The deltoid muscle was measured using a spherical ROI in Leitner et al 2017. As we have described above, the purpose of skeletal muscle quantification in that paper was beyond of the scope of this manuscript.

2. An important result of this study is to add some information about which is the average time to analyse 1 participant. ***We added a sentence in discussion: "The time it takes to complete analysis of a single scan can range from three to eight hours, which gets shorter with practice and experience."***

3. Other interesting results are how to calculate the total BAT parameters after the delimitation of ROIs.
While we agree with this comment in principle, we believe that, due to the different needs of potential users, it is hard to answer this question with any specificity. We therefore did not include a step on post-processing data analysis because it is out of the scope of this manuscript.

DISCUSSION:
1. It should be mentioned as a limitation that this protocol is time consuming, specially for large intervention studies.
Addressed. See concern #2 in RESULTS section above.

2. I agree that 18F-FDG is the most used method to quantify BAT, however this protocol should be replicated in studies using other tracers, for instance 18F-FTHA.
We agree with the reviewer that such a replication would be extremely important for the field. However, our group does not perform BAT studies with any other tracer than 18F-FDG. For this reason we have clarified throughout the text (beginning with the title) that the quantification demonstrated here has been done only with 18F-FDG.

Minor Concerns: Abstract:
- Lines 31-32: It is stated that "BAT´s ability to expend energy highlight a potential target for novel therapies to ameliorate obesity and associated metabolic disorders in humans"… However this affirmation should be toned down ("might highlight a potential target"), and it should be noted that not only the BAT´s capacity to expend energy is a potential target for novel therapies, but also its endocrine role in human metabolism.
Thank you, we have reworded the sentence and eliminated the word "highlight" to tone down the sentence. We agree that the endocrine roles of BAT are likely to have substantial influences on human metabolism as well, but for brevity and clarity, we have not included descriptions regarding such roles.

Introduction:
- What about the dose use for PET and CT? It is of interest to mention in the introduction that this issue could reduce the overlapping of the PET over the CT.
This method has been used by our group on multiple doses of both PET and CT scans. Because these factors are likely to vary across all groups that use this method, we have opted not to introduce any confusion that may lead readers to believe that this analysis is limited by the PET and CT dosages of the scans obtained.

- Line 50: It is mentioned that "obesity is attributed to an excess of white adipose tissue (WAT), which stores energy in the form of triglycerides". This sentence might be too simplistic.
We agree, there are many factors that contribute to obesity and we have adjusted the text to reflect this. The text now reads: "Obesity is due in part to excess energy stored in the white adipose tissue (WAT) in the form of triglycerides[2]"

- Line 52: BAT also presents a larger innervation…
- Line 56: "…ATP", long

Thank you for these suggestions, we have adjusted the first sentence and shortened the section as suggested. The sentences now read: "Brown adipose tissue (BAT) differs from WAT most notably due to its higher mitochondrial content, smaller, multilocular lipid droplets, distinct anatomical distribution, greater sympathetic innervation, and heat generating ability"

- Lines 61-63. These correlations have been reported. However, not consistently (e.g. Blondin et al. 2015 J Phys, Bakker et al. 2014 Lancet End Metab; Lee et al Diabetes 2014). Please state it.
Agreed. We thank the reviewer; the appropriate citations have been added.

- Line 68: It is stated that "the precise measurements are challenging due to BAT´s unique anatomic location in humans". This sentence should be modified since it could lead to the equivocal believe that BAT is located in a unique anatomical location in humans. In the following sentence (lines 69-70), you properly mention how BAT is distributed through the neck, thorax and abdomen.

Agreed. As suggested, we changed the word "location" to "distribution".

- Line 74: "This heterogeneity also makes automatic quantification of BAT more difficult than homogenous structures such as the liver" this sentence needs reference.
The reference by Chauvie et al, 2018 in Computer Methods and Programs in Biomedicine has been added to support this claim.

- Line 78: "The radiolabeled glucose analog 18F-Fluourodeoxyglucose (18F-FDG) is the most widely used tracer to study metabolic activity in BAT". This sentence needs reference (e.g. PMID: 29119565)
Thank you for the suggestion. We used the study provided by the reviewer as the reference.

- Lines 88-89. You explain how patient motion can affect to the overlapping of both PET and CT images. It would be desirable to mention in the limitations paragraph that the method that you are proposing still have to face with this limitation.
The reviewer is correct. We have moved this paragraph to the discussion as suggested by the editor and we have also included that this is a limitation to our method in a separate limitation paragraph of the discussion.

Protocol
- Figure 3, should be figure 1 because is the first figure that has been mentioned in the text.
We agree and have changed the order of the figures.

- Please, explained what is a DICOM file when is the first time that is mentioned.
We have added a note in the text that clarifies what is meant by "Dicom image"

and "DICOM Path". The NOTE for this section now reads: "a DICOM (Digital Imaging and Communications in Medicine) is a file format commonly used for medical images and the "DICOM path" refers to the set of folders that contains all raw DICOM images."

- 3.1.2. The order of images that will appear in FIJI is firs PET, CT and Fusion and I will show a screenshot of this.
This will be shown in the video. Excess screenshots have not been added to the figures because the video will provide much richer information than many screenshots.

- Line 180: change "Brown fat ROIs" by "Brown fat, ROIs".
Addressed.

- Line 189: I will show to readers a screenshot of the "Brown fat, ROIs" option.
This will be shown in the video. Excess screenshots have not been added to the figures because the video will provide much richer information than many screenshots.

- Line 211: Please refer to PMID 29867076 and discuss.
Thank you for the suggestion, a line has been provided to refer users to PMID 29867076, and the citation has been added.

- In the section: 3.9.2.1: slice limits: Please, explain how to do that.
Thank you for the suggestion. We modified the text to clarify this step, but we hope that the video will provide additional clarity: "Set the starting and ending "slice limit" to the same slice, so that the ROI will only apply to the current axial slice (e.g. starting slice = 90 and ending slice = 90)."

- Line 300: etc and … is the same. Please only use one, I would recommend etc.
It is not the same. We have attempted to make the distinction between the two types of deleting clearer.

- Line 331: "Thyroid and BAT have the same density". Please reference this assumption. To my knowledge, there is no paper published concluding a definitive radiodensity of thyroid.
We agree with the reviewer. In order to refrain from certainty regarding the densities of BAT and thyroid, we have changed that sentence to: "Exclude the thyroid, which may have similar density and activity level as BAT"

- It is important to stablish that Fiji software is in continuous development and the actualization of this software are automatic, however the researcher needs to update the software every time that they observe the message of update.

To address this point, we have added to our sentence that directs the user to petctviewer.org, where all updates affecting the PET CT Viewer can be found. (Section 1.2)

REVIEWER #2 COMMENTS:

Major Concerns:

L92: The authors should clarify what they mean by "user specified regions".
We now clarified it to read: "one should apply PET and CT criteria only within the regions of interest (ROIs) that users construct" **Note that this paragraph has been moved to the second paragraph of the discussion section per the editor's instructions.**

L96: Would the ROIs be drawn on every slice based on experience, the literature, or some other source?
We believe that the ROIs should be drawn on every axial slice where active BAT is found based on experience and literature. Although our revised paragraph does not include this statement based on the instructions by the Editor, we hope that this point is made clear in other sections and in the final video.

L197: The authors refer to "more lenient voxel inclusion". Doesn't this broader selection of voxels create more false positives?
Similar to our previous response to Reviewer 1, we clarified that this option should be made by the user. The revised statement is now in Section 5.ii.

L198: The new/innovative component of this method is not clear. Please, add some more information.
Thank you for the comment. We revised the introduction and discussions to clarify our aim for this work.

L210-212: Don't we have BARCIST for that?
The reviewer is correct. We have revised this section to simplify it.

L214: Shouldn't the authors provide a threshold here? They should also define how this threshold is determined.
The reviewer is correct and we have reorganized the sentence to make the upper threshold recommendation based on our previous publication.

L237: It would be helpful for the reader if the authors explain why that would be the case.
We revised this section to address this point by adding "NOTE: It is easiest to

have a maximum of one ROI per axial slice. Including more than one ROI per slice may lead to inadvertent overlap. Voxels identified as BAT in overlapping regions would then be counted more than once toward total BAT volume". It is now in section 3.10.i.

L240: What does "commonly" mean? Is it not always the case?
Thank you for the comment. This has been revised and removed.

L288-290: Does this refer to identification that the user has done on their own?
Yes, this is to visualize the confirmed BAT. We now clarify this in the revision to read "Check the checkbox located beneath "Vol*mean" so that all voxels deemed to be BAT will be highlighted in blue while the "brown fat, ROI" window is open. NOTE: The SUVmax will appear in red and the adjustable number next to this checkbox dictates the thickness of the highlight." This is now moved to section 3.8.

L438: Why is this change to the lower limit needed?
We have restated this to read "Uncheck the density (HU) threshold and change the lower limit of the PET (SUV) threshold to 0.01 SUV to exclude any non-BAT voxels which now have an SUV value of 0." This is now in section 6.2.iii.

L510-511: Does this mean that everything is done according to the BARCIST?
We believe that only users who are interested in performing regional BAT analysis will be knowledgeable in this area. Thus, we removed this statement.

L519: Does this mean that there is also shivering thermogenesis involved?
It is certainly possible that when there is 18F-FDG uptake in skeletal muscle that shivering thermogenesis is occurring. The purpose of this protocol is to focus on quantifying active human BAT, but we now added a paragraph in the discussion addressing this.

L520: The authors refer to "highlighted several common regions… supraclavicular BAT vs. shivering muscle near borders of air and solid tissue". Does this mean that this was not done thus far?
We apologize for the lack of clarity in this part of the text. We did not mean highlight in the way that this protocol was the first to show common false positives. We revised this section to bring more clarity.

L606-612: The authors should consider briefly indicating the innovative/different component as compared to existing analyses.
Thank you for the comment. It is our view that, while this method is not necessarily innovative as we and others have been using it, the step-by-step instructions on how to use the software for BAT quantification do not exist.

Furthermore, the JOVE video provides the unique ability to visually demonstrate how to accomplish this, which cannot be fully explained in written instructions.